Effect of Antenna Polarization on the Capacity of a Multiple Element System in an Indoor Environment

Persefoni Kyritsi, *Student Member, IEEE,* Donald C. Cox, *Fellow, IEEE,* Reinaldo A. Valenzuela, *Fellow, IEEE,* and Peter W. Wolniansky

***Abstract*—In this paper, we analyze the behavior of a multiple element antenna system in an indoor environment based on the measurements taken in the Lucent Bell Labs building in Crawford Hill, NJ, with a system of 12 transmitters and 15 receivers. In particular, we investigate the capacity behavior with respect to the polarization of the transmitting/receiving elements and the distance between the transmitting and the receiving arrays.**

The analysis of the power rolloff versus distance clearly demonstrates the different propagation characteristics of the horizontally versus the vertically polarized electric fields. Under strong line-of-sight (LOS) conditions (hallway environment), the power of the horizontally polarized waves falls off faster with distance than that of the vertically polarized fields. Also, the cross-polarization coupling is about −15 dB. Under nonline-of-sight (NLOS) conditions (labs), both polarizations display similar rolloff behavior with distance and the cross-polarization coupling is about 0 dB. There is a power loss of at least 15 dB under NLOS conditions relative to LOS conditions.

The average received signal power affects the system capacity. In the hallway, horizontally polarized systems achieve lower capacities than their vertically polarized counterparts. Also the achievable capacity in the labs is much lower than that in the hallway, because of the lower average received power.

The comparison of single polarization systems to hybrid polarization systems shows that combined polarization systems perform better in terms of achievable capacity. Therefore, there lies an advantage in using both electric field polarizations. However, under strong LOS conditions the channel itself inherently limits the capacity behavior of the system.

***Index Terms*—Diversity methods, indoor propagation, multiple-input/multiple-output systems, polarization, radio propagation, wireless local area network.**

I. Introduction and Motivation

In recent years, a lot of attention has been drawn to systems with multiple element transmitter and receiver arrays, because they can achieve very high spectral efficiencies [1]. This is particularly significant for wireless applications that are power, bandwidth, and complexity limited.

Assume a system with M transmitters and N receivers. Each transmitter sends an independent data stream of power E_x, so that the total transmitted power is $P_t = ME_x$. Let $\underline{x}$, $\underline{y}$ be the transmitted and the received signal vectors, respectively. In the case of a flat-fading channel (no variation with frequency), the channel gain from transmitter j to receiver i is a scalar quantity, denoted T_{ij}. The transmitted and received signals are related by the equation $\underline{y} = \mathbf{T}\underline{x} + \underline{n}$.

The matrix $\mathbf{T}$ (channel transfer matrix) incorporates the channel transfer gains from each transmitter to each receiver.

$\underline{n}$ is the receiver noise vector. It is assumed that the noise at the receivers is Gaussian, of equal power σ^2, and its components are independent of each other, so that the noise auto-correlation matrix is $\mathbf{R}_{\underline{nn}} = \sigma^2\mathbf{I}$ ($\mathbf{I}$: identity matrix).

The generalized Shannon capacity for this channel is given by the formula

$$C = \log_2\left(\det\left(\mathbf{I} + \frac{E_x}{\sigma^2}\mathbf{T}\mathbf{T}^H\right)\right) \tag{1}$$

where $\mathbf{T}^H$ is the Hermitian (complex conjugate transpose) of the matrix $\mathbf{T}$.

All the signals used in our formulation are discrete-time complex baseband, so the vectors $\underline{x}$, $\underline{y}$, $\underline{n}$ and the elements of the channel transfer matrix $\mathbf{T}$ are complex. It is assumed that perfect down conversion, filtering, and sampling have been performed.

The capacity of (1) is the maximum data rate that can be achieved over this channel under the previous assumptions. Complexity (coding, detection) and constellation size constraints limit the data rates that can be attained with a real-life system. However, several techniques that require advanced signal processing at the receiver have been developed and have been demonstrated to achieve a hefty portion of the theoretically achievable capacity [2].

The initial theoretical studies assume certain statistical properties for the entries of the channel transfer matrix $\mathbf{T}$. A common assumption is that of independent Gaussian distributed elements, as in the case of a rich scattering scenario, which results in a channel capacity that scales linearly with the number of transmitting/receiving elements. On a more practical level, the actual channel has to be measured. This paper describes the measurements that were taken in the Lucent Bell Labs building in Crawford Hill, NJ, with a system of 12 transmitters and 15 receivers. The goal of the measurement campaign was to study the dependence of the channel capacity on the distance between the transmitter and the receiver arrays in two different environments (under strong/weak line-of-sight (LOS) conditions in the hallway/in the labs, respectively).

The results for the entire system have been presented in [4]. They describe the behavior of the system as a whole and do not study the performance dependence on polarization. However,

Manuscript received March 15, 2001; revised September 27, 2001 and February 11, 2002. This work was supported in part by Lucent Technologies. This paper was presented in part at the Wireless Communications and Networking Conference (WCNC) 2002 in Orlando, FL.

P. Kyritsi is with the Center for PersonKommunikation, Aalborg, DK-9220 Denmark (e-mail: persa@cpk.auc.dk).

D. C. Cox is with the Department of Electrical Engineering. Standord University, Stanford, CA 94305-9515 USA (e-mail: dcox@spark.stanford.edu).

R. A. Valenzuela and P. W. Wolniansky are with the Bell Labs, Lucent Technologies, Holmdel, NJ 07733 USA (e-mail: rav@lucent.com; pww@lucent.com).

Publisher Item Identifier 10.1109/JSAC.2002.801225.

0733-8716/02$17.00 © 2002 IEEE

TRANSMITTER SIDE

V_1	H_6	V_6	H_5
H_1			V_5
V_2			H_4
H_2	V_3	H_3	V_4

RECEIVER SIDE

H_5	V_6	H_6	V_1
V_5	H_8		H_1
H_4	V_7	H_7	V_2
V_4	H_3	V_3	H_2

Fig. 1. Antenna array layout.

it is known that the different electric field polarizations have different propagation characteristics [3].

Moreover, the study of the 12×15 system capacity showed that the system capacity does not scale linearly with the number of elements, as one would have expected in a rich scattering environment. This indicates that the signals are highly correlated. Indeed, in the hallway, the strong LOS component and the narrow angular spread increase the signal correlation and limit the effective rank of the channel transfer matrix, so that the ideal capacities cannot be achieved. The experience of diversity systems has shown that wider element spacing results in higher signal decorrelation, which would increase the channel capacity. The question is how much the performance improves given higher interelement separation (lower correlation).

Finally, the measurements were taken with a system of 12 transmitters and 15 receivers. Each one of the elements included an antenna and a radio chain and the signals to all the transmitters and from all the receivers were processed in two independent signal-processing units. A system of such dimensions and complexity is not practical for real-life commercial applications because of the limitations inherent in a wireless system. The hardware cost (mainly in the radio chain), the volume of the device (proportional to the number of antennas used and the wavelength), and power consumption (in the form of transmitted power or for the signal processing) suggest that a lower number of elements should be used.

For those reasons (polarization effect on propagation characteristics, diversity benefit of wider spacing, and cost efficiency), we study the performance of 4×4 single/hybrid polarization multiple antenna systems. This paper is organized as follows. Section II describes the measurement equipment and the measurement process. Section III describes the power rolloff in both environments. Section IV introduces the subsystems that we will study. Section V analyzes the capacity dependence on distance and polarization under the assumption of constant transmitted power and Section VI shows the system capacity behavior for a reference signal-to-noise ratio (SNR). Section VII contains the conclusions of our analysis.

II. Measurement Process

The purpose of the experiment was to study the dependence of the channel transfer matrix $\mathbf{T}$ on the distance from the transmitter, the orientation of the receiver, and the propagation environment (hallway versus labs).

A. Description of the Measuring Equipment

The measurements were taken with two antenna arrays: the transmitter array comprised 12 elements arranged on the sides of a square and the receiver array comprised 15 elements arranged in a grid. Adjacent antennas were separated by 8 cm and the elements on both sides were arranged with alternate polarizations. Fig. 1 shows the transmitter and the receiver array as seen from the front. V (H) stands for vertically (horizontally) polarized elements.

The two arrays were placed at a height of 2 m. The antennas were folded cavity backed slot elements mounted on $2' \times 2'$ panels. This type of antenna is not omni-directional, but its gain pattern is close to a hemisphere. The operating frequency was 1.95 GHz. The system bandwidth was 30 kHz, the filters were raised cosine filters with a bandwidth expansion factor of $\alpha = 0.23$, which meant that the symbol rate was 24.3 ksymbols/s. The constellation size used was four quaternary phase-shift keying (QPSK). A cable connecting the two arrays provided synchronization between the transmitter and the receiver.

B. Measurement Location

The measurement campaign was conducted in the Lucent Bell Labs building in Crawford Hill, NJ. This is a two-story building that houses approximately 150 people and is built on the side of a hill. On the front side there is a parking area and on the back side of the building, at a distance of approximately 100 ft, there is the hill slope.

The outside walls of the building are largely glass, whereas the inside walls are made of wood and wallboard. The ceilings and the floors are made of reinforced concrete over steel plates. The measurements were taken on the second floor of the building, in the main corridor, and in the adjacent labs. The main corridor is a straight hallway, 390 ft long, 6 ft wide, and 10 ft high. The hallway is lined with offices (typically 10 ft $\times$ 10 ft) on one side and laboratories (typically 12 ft $\times$ 24 ft) on the other. The offices face the parking lot and the labs face the side of the hill. There is a second corridor that intersects the first one in a T shape. The second corridor is also lined with rooms, but no measurements were taken in that environment. The labs measurements were taken in the laboratories adjacent to the primary hallway. A rough layout of the building is shown in Fig. 2. In reality, the building extends on both sides.

For all our measurements the transmitter was placed 82.5 ft from one end of the hallway (0° direction) and 2 ft from the northern wall of the hallway (90° direction), facing west (180° direction). This point is the origin (0,0) of our axis system. The receiver was wheeled to the desired position for each measurement and data were collected.

In the hallway, the receiver was wheeled to the desired position at distances between 3 ft and 246 ft from the transmitter at 3 ft intervals. Wherever possible, the receiver was placed at the

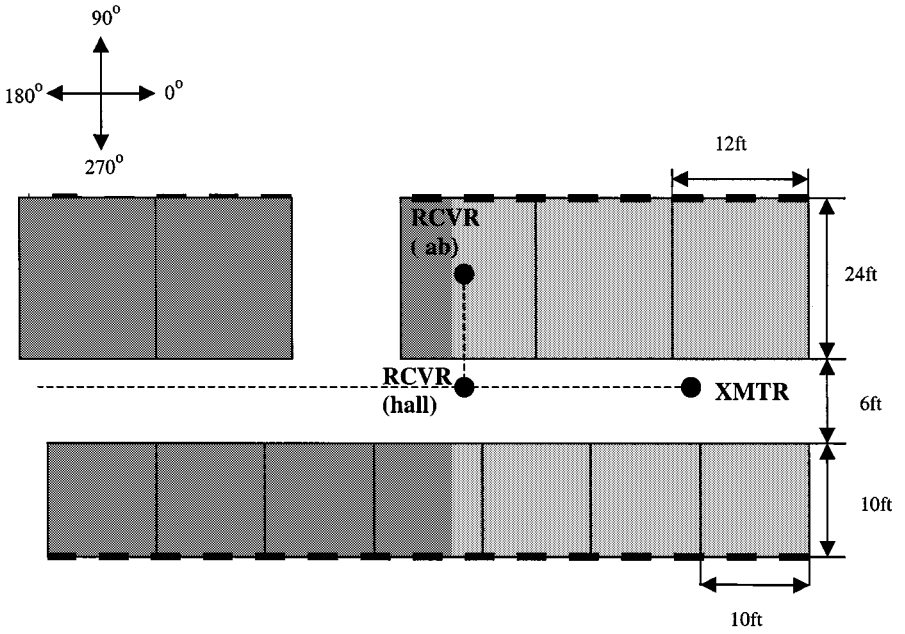

Fig. 2. Building layout.

same distance from the hallway walls as the transmitter. When this was not possible, the maximal receiver displacement was 1 ft from the nominal location. A total of 82 locations were measured in the corridor.

In the labs, the receiver was again wheeled to the desired position, which was 8 ft north, perpendicular to the 0°–180° line in the hall defined by the transmitter. Measurements were taken in 11 labs.

Along the hallway, measurements were taken with the receiver facing toward the transmitter (0° orientation). In the labs, measurements were taken for all four orientations (0°, 90°, 180°, and 270°).

C. Description of the Measuring Process

The prototype used for the measurement campaign processes data in bursts. Each burst consists of 100 symbols. Out of these, the 20 first symbols are training symbols and are used for the measurement of the channel transfer matrix. This is performed with orthogonal training sequences as described in [6]: during the training phase each antenna transmits a row of a $M \times L$ $(= 12 \times 20)$ Fourier matrix (orthogonal rows), appropriately scaled to the transmit power. At the receiver side, the channel estimation is performed by applying the pseudo inverse of the transmitted training matrix to the received training matrix. The last 80 symbols of each burst are data symbols that are decoded using the Bell Labs Layered Space-Time (BLAST) algorithm [2]. These 80 data symbols are not used in this analysis. We are interested in the channel characteristics so we concentrate on the recorded channel transfer matrices.

The transmit power during the signal measurements was set to 9.2 dBm for most locations, except for the measurement points in the hallway at distances 3 ft to 18 ft. The close locations require lower transmit power to prevent receiver saturation. The results that we present have been compensated for the lower transmitted power at the small distances.

At each measurement location, about 100 bursts (100 temporal samples of the channel transfer matrix $\mathbf{T}$) were recorded in order to average over the small scale temporal variation (doors opening and closing, people walking through the hallway, or in the labs, etc). Also, the average SNR at all locations was at least 15 dB. This was done in order to guarantee the accuracy of the capacity calculation [7].

D. Capacity Calculation

Previous measurements in the same environment have shown that the maximum delay spread τ_{MAX} is less than 0.8 μs [5]. The symbol time T_s was 41 μs. So $T_s > \tau_{\mathrm{MAX}}$ and the narrowband assumption holds.

Following the analysis of Section I, we define the average channel gain g as

$$g^2 = E\left[|T_{ij}|^2\right]. \tag{2}$$

We can define the normalized channel transfer matrix $\mathbf{H}$ as

$$\mathbf{T} = g\mathbf{H} \tag{3}$$

and the average SNR ρ as

$$\rho = \frac{P_t}{\sigma^2} g^2. \tag{4}$$

Similarly to the Shannon formula for the single transmitter/single receiver case, the channel capacity can be expressed in terms of the average SNR ρ as

$$C = \log_2\left(\det\left(\mathbf{I} + \frac{\rho}{M}\mathbf{H}\mathbf{H}^H\right)\right). \tag{5}$$

Therefore, for a given channel transfer matrix $\mathbf{T}$, the capacity of the channel can be calculated for any arbitrary reference SNR ρ_{ref} by using the normalized channel transfer matrix $\mathbf{H}$

$$C_{\rho_{\mathrm{ref}}} = \log_2\left(\mathbf{I} + \frac{\rho_{\mathrm{ref}}}{M}\mathbf{H}\mathbf{H}^H\right). \tag{6}$$

For a given reference SNR and system size, the channel capacity is maximized when the matrix $\mathbf{H}$ is unitary. In practice, the channel transfer matrix is not unitary and the statistics of its elements depend on the propagation environment.We present the results for the capacity of the measured channel in the two environments. This capacity is calculated based on the recorded channel transfer matrix using (1) and (6) and is, therefore, the calculated capacity of the measured channel. More specifically we show the two following quantities.

a) The capacity of the measured channel for a reference noise level as per (1) (we select $\sigma^2 = -97.5$ dBm, which is close to the actual noise level during the measurements). This quantity shows how the change in both the average signal power and channel characteristics affects the channel capacity.
b) The capacity for the reference SNR ($\rho_{\text{ref}} = 20$ dB) as per (6). This quantity isolates the effect of the signal power rolloff with distance and concentrates on the effect of the channel change. An alternative way to think of this approach is in terms of power control: at every measurement point, the transmitted power is set to such a value that the average received SNR is 20 dB.

III. Power Dependence on Polarization and Distance

We study how power couples between transmitters and receivers of the same polarization and between cross-polarized elements.

The sets of vertically and horizontally polarized elements on each end of the communications link are defined as (V: vertical, H: horizontal):

$$\left\{ \begin{array}{l} V_{\text{XMTR}} = \{V \text{ polarized transmitters}\} \\ H_{\text{XMTR}} = \{H \text{ polarized transmitters}\} \end{array} \right\}$$
$$\left\{ \begin{array}{l} V_{\text{RCVR}} = \{V \text{ polarized receivers}\} \\ H_{\text{RCVR}} = \{H \text{ polarized receivers}\} \end{array} \right\}$$

In this case, the average received power for each polarization combination is defined as

$$\bar{P}_{VtoV} = \frac{1}{|V_{\text{XMTR}}|\,|V_{\text{RCVR}}|} \left(\sum_{i=1}^{|V_{\text{RCVR}}|} \sum_{j=1}^{|V_{\text{RCVR}}|} |T_{ij}|^2 \right) P_T$$
$$j \in V_{\text{XMTR}}, i \in V_{\text{RCVR}}$$
$$\bar{P}_{HtoH} = \frac{1}{|H_{\text{XMTR}}|\,|H_{\text{RCVR}}|} \left(\sum_{i=1}^{|H_{\text{RCVR}}|} \sum_{j=1}^{|H_{\text{RCVR}}|} |T_{ij}|^2 \right) P_T$$
$$j \in H_{\text{XMTR}}, i \in H_{\text{RCVR}}$$
$$\bar{P}_{VtoH} = \frac{1}{|V_{\text{XMTR}}|\,|H_{\text{RCVR}}|} \left(\sum_{i=1}^{|H_{\text{RCVR}}|} \sum_{j=1}^{|V_{\text{RCVR}}|} |T_{ij}|^2 \right) P_T$$
$$j \in V_{\text{XMTR}}, i \in H_{\text{RCVR}}$$
$$\bar{P}_{HtoV} = \frac{1}{|H_{\text{XMTR}}|\,|V_{\text{RCVR}}|} \left(\sum_{i=1}^{|V_{\text{RCVR}}|} \sum_{j=1}^{|H_{\text{RCVR}}|} |T_{ij}|^2 \right) P_T$$
$$j \in H_{\text{XMTR}}, i \in V_{\text{RCVR}}.$$

The study of the 12×15 system [4] showed that the power rolloff law is different in the hallway from what it is in the labs. For this reason, we study these two environments separately. The fact that the antennas are not colocated offers some spatial averaging over the vertical spatial cross section of the environment.

A. Power Versus Distance in the Hallway

Fig. 3 shows the average received power in the hallway versus distance for the different polarization combinations. We have also performed a least-squares fit to the measurement curves for functions of the form $d^{-\gamma}$ and $e^{-\alpha d}$ (d being the distance from the transmitter array). The dashed lines represent the $e^{-\alpha d}$ and the dotted lines represent the $d^{-\gamma}$ fits.

The power for horizontally polarized transmitter-receiver pairs falls off faster with distance than for vertically polarized transmitter-receiver pairs. This is more clearly seen in the fitted curves and has been extensively analyzed in [8]: it is due to the different reflection coefficients for the different polarizations. The floor and the ceiling can be represented by a high dielectric constant or as conducting materials, in which case the reflection for both polarizations is high. The walls are better approximated as dielectric materials. The waves that have polarization parallel to the walls (horizontally polarized) undergo a Brewster angle phenomenon and penetrate the walls without any reflection at all. At angles near the Brewster angle the reflection is not zero but greatly reduced. No such effects are present for the vertical polarization (perpendicular with respect to the walls).

Table I shows the reflection coefficient as a function of the polarization of the incident wave and the properties of the reflecting surface, assuming that the permittivity constant of the material in the hallway is that of free space.

Power for cross-polarized transmitter-receiver pairs falls in similar ways for both polarizations. Cross-polarization coupling is about -15 dB, which is consistent with previous measurements in the same environment [10].

The functions $d^{-\gamma}$ and $e^{-\alpha d}$ to which the measured data have been fitted correspond to different power decay laws. The values of the parameters γ, α and the corresponding errors (ε_γ and ε_α) in the curve fitting are shown in the Table II. We observe that the power rolloff is better approximated by a law of the form $e^{-\alpha d}$, which relates to distributed losses in one dimensional propagation as in the environment of a lossy waveguide. What we graphically observed for the faster rolloff of the horizontal to horizontal combination compared with the vertical to vertical combination is verified by the curve-fitting parameters. We also noticed graphically that power rolls off in similar fashions for the cross-polarized pairs and this again is verified by the curve-fitting parameters.

B. Power Versus Distance in the Labs

Fig. 4 shows the average received power in the labs versus the distance from the transmitter. The added parameter is the antenna orientation. As a reference the hallway measurements are also shown.

The labs curves are not as smooth as the hallway curves. This is due to the limited number of labs measurements (11 locations), relative to hallway measurements (82 locations), and the greater separation of the measurement locations. Moreover, the

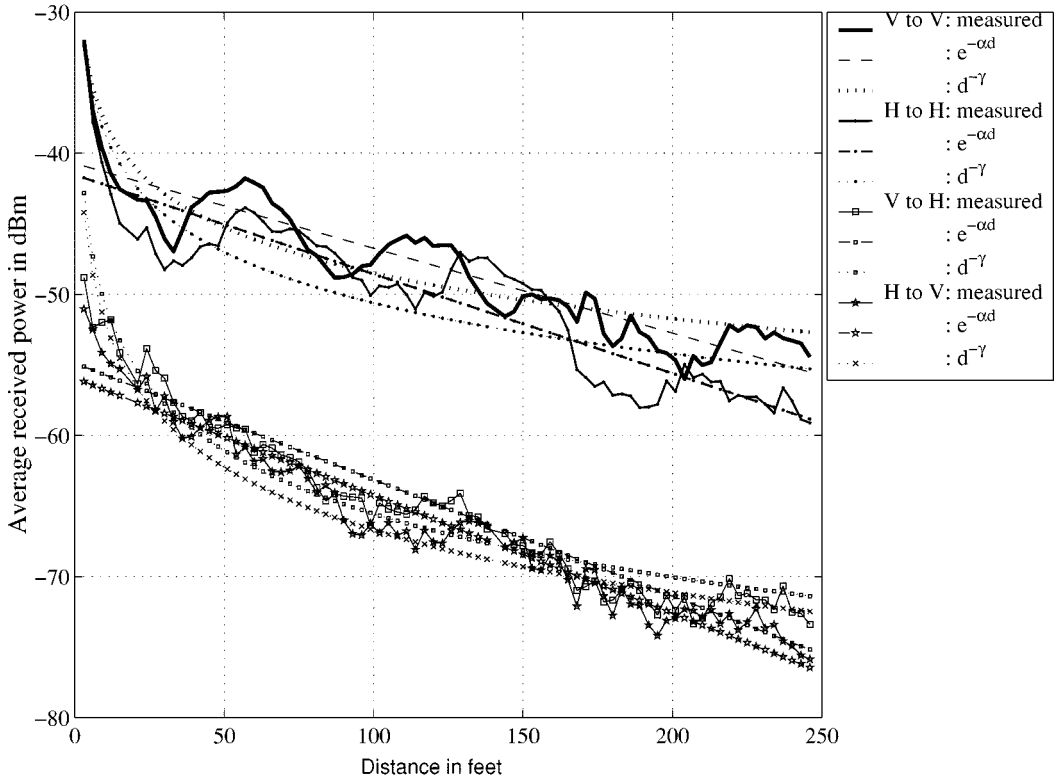

Fig. 3. Power versus distance and polarization for 0°-oriented receivers in the hallway.

TABLE I
REFLECTION COEFFICIENT WITH RESPECT TO POLARIZATION AND DIELECTRIC/CONDUCTING PROPERTIES OF THE REFLECTING SURFACE (ε_r: RELATIVE DIELECTRIC CONSTANT)

	Perfect conductor	Dielectric	Brewster angle
Horizontal polarization (// walls)	1	$\dfrac{\varepsilon_r \cos\theta_i - \sqrt{\varepsilon_r - \sin^2\theta_i}}{\varepsilon_r \cos\theta_i + \sqrt{\varepsilon_r - \sin^2\theta_i}}$	Yes $\theta_B = \tan^{-1}(\varepsilon_r)$
Vertical polarization (⊥ walls)	-1	$\dfrac{\sqrt{\varepsilon_r - \sin^2\theta_i} - \cos\theta_i}{\sqrt{\varepsilon_r - \sin^2\theta_i} + \cos\theta_i}$	No

TABLE II
CURVE FITTING PARAMETERS IN THE HALLWAY WITH RESPECT TO POLARIZATION

		α (ft^{-1})	ε_α (dB)	γ	ε_γ (dB)
0°	$P_{V\text{ to }V}$	0.0138	1.5106	1.0728	1.6553
	$P_{H\text{ to }H}$	0.0162	1.7274	1.1957	2.5854
	$P_{V\text{ to }H}$	0.0190	1.3495	1.4908	1.4100
	$P_{H\text{ to }V}$	0.0192	1.2256	1.4769	1.5278

power behavior is not smoothly decreasing with distance. For example, power seems to be higher around 140 ft than around 120 ft. This is due to the standard deviation of indoor power measurements.

There is a loss of at least 15 dB relative to the 0° orientation at short distances in the hallway and the difference between the hallway and the lab curves increases with antenna separation.

We cannot infer that one or the other polarization combination rolls off significantly faster with distance. In contrast to the hallway measurements, the coupling between the two polarizations is much more significant in the labs because of scattering from indoor clutter and oblique reflections from the walls. Moreover, the cross-polarization coupling is in the order of 0 dB.

For a given polarization combination, all antenna orientations in the labs have similar behaviors. The orientation that achieves the lowest received power is the 90° one, because the receivers pointing toward the glass windows mainly pick up power that

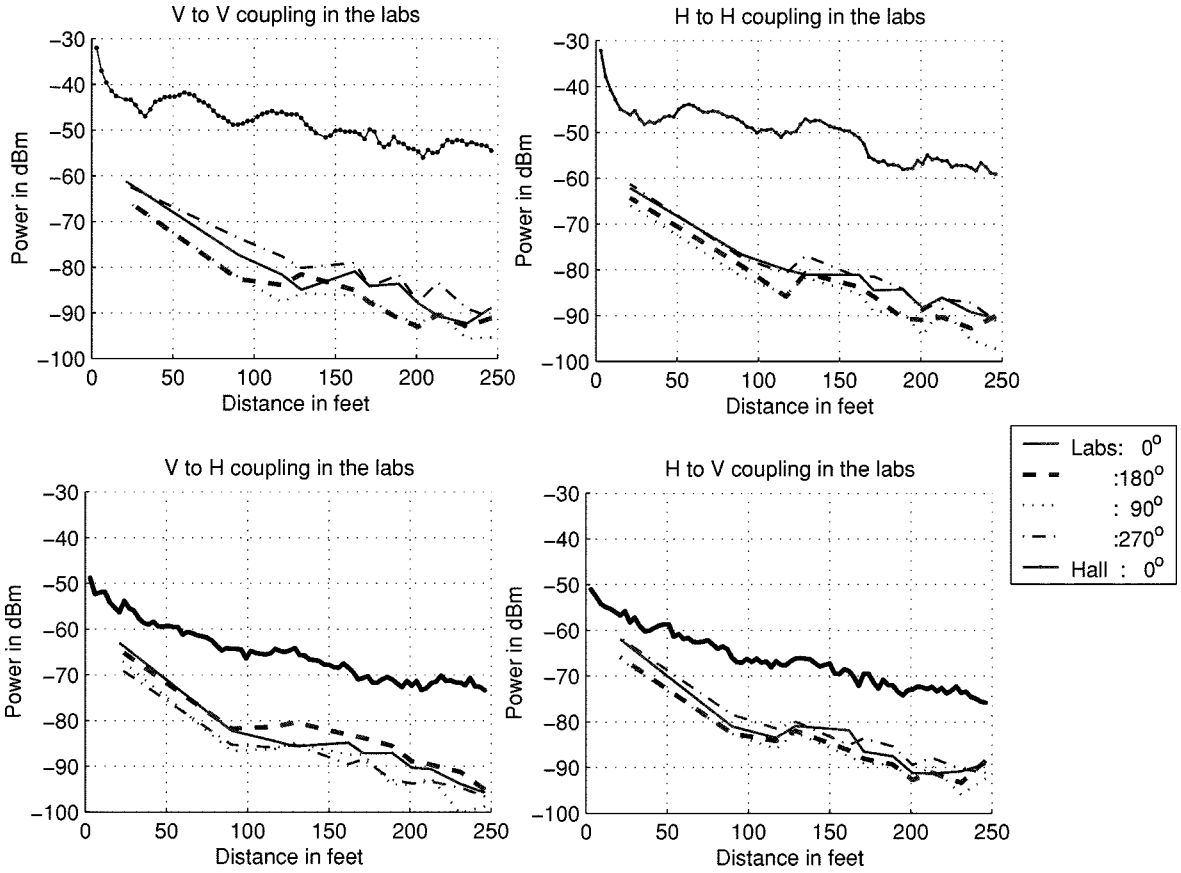

Fig. 4. Power rolloff with distance in the labs.

has been reflected off the hill in the back of the building and has been significantly attenuated.

The fact that there is high cross-polarization coupling and that the average received power is independent of the receiver orientation supports the claim that there are rays arriving from all directions.

As with the hallway measurements, we have performed least-squares fits to the measured data with functions of the form $d^{-\gamma}$ and $e^{-\alpha d}$. Table III summarizes the resulting curve-fitting parameters α and γ and the associated errors ε_α and ε_γ. It is clear that a function of the form $d^{-\gamma}$ is a better fit to the measurements. The average value of the parameter γ of the exponential rolloff is 2.64.

In general, we can classify the signal paths into the labs into two broad categories:

1) down the hallway and through the door;
2) through the walls.

At the short distances, both kinds of signal paths into the labs suffer similar attenuation and are, therefore, of comparable strengths. At larger distances the dominant propagation path to the labs is down the hallway and through the door. The power rolloff law in the hallway determines the power rolloff for the first part of the path.

To these paths local scattering in the labs (due to furniture, cabinets, shelves, partitions, walls, etc.) is superimposed. The existence of such reflecting surfaces in the lab environment as well as the fact that the power measurements are similar for all antenna orientations indicate that indeed in the labs signals reach the receivers with a uniform angle of arrival. The compound effect is experimentally shown to be better approximated as a $d^{-\gamma}$ function of distance from the transmitter.

IV. Subsystem Selection

We study the transmitter and receiver arrays of Fig. 1. For reasons of fairness and symmetry, we concentrate on the 12 receivers on the edges of the receiver array. They maximize the inter-element separation for their subsystems and are symmetrical for both polarizations.

We look at the following 4×4 single polarization subsystems that maximize the vertical and horizontal separation, respectively:

- Vertical polarization: $Iv = \{V_1, V_3, V_4, V_6\}$ and $IIv = \{V_1, V_2, V_4, V_5\}$.
- Horizontal polarization: $Ih = \{H_2, H_3, H_5, H_6\}$ and $IIh = \{H_1, H_2, H_4, H_5\}$.

We compare these to the 4×4 subsystem HV that comprises the corner antennas of both squares: $HV = \{V_1, H_2, V_4, H_5\}$.

The channel capacity is calculated from the Shannon formula using the measured value of the channel transfer matrix. In each case, we select the appropriate submatrix. We first study the subsystem capacity behavior for constant transmitted power (i.e., using the channel transfer matrix $\mathbf{T}$) and then for constant reference SNR (i.e., using the normalized channel transfer matrix $\mathbf{H}$).

TABLE III
CURVE FITTING PARAMETERS IN THE LABS WITH RESPECT TO POLARIZATION

		α (ft^{-1})	ε_α (dB)	γ	ε_γ (dB)
0°	$P_{V\,to\,V}$	0.0268	10.3038	2.9411	4.8164
	$P_{H\,to\,H}$	0.0259	4.6039	2.5560	2.0165
	$P_{V\,to\,H}$	0.0263	10.3038	2.7921	2.9411
	$P_{H\,to\,V}$	0.0277	14.9703	2.6942	3.9160
180°	$P_{V\,to\,V}$	0.0256	8.1742	2.5740	3.4376
	$P_{H\,to\,H}$	0.0260	8.4558	2.6020	4.1644
	$P_{V\,to\,H}$	0.0254	5.1088	2.5165	1.9102
	$P_{H\,to\,V}$	0.0239	10.4618	2.4415	3.4509
90°	$P_{V\,to\,V}$	0.0266	8.4332	2.6788	3.1442
	$P_{H\,to\,H}$	0.0281	7.1471	2.7101	6.9159
	$P_{V\,to\,H}$	0.0293	9.4363	2.8512	7.8247
	$P_{H\,to\,V}$	0.0252	8.0935	2.5260	3.1184
270°	$P_{V\,to\,V}$	0.0268	4.7819	2.5440	5.9569
	$P_{H\,to\,H}$	0.0264	6.3348	2.583	4.3032
	$P_{V\,to\,H}$	0.0262	5.5137	2.5179	5.4811
	$P_{H\,to\,V}$	0.0264	8.3939	2.6893	1.7059

We assume the total transmitted power to be the same as for the original array ($P_t = -9.2$ dBm). For each subsystem it is equally divided among its transmitters. The implication that is not taken into account in this calculation is that higher transmitted power per transmitter would require new transmitter and receiver design in order to raise the saturation levels.

V. CAPACITY MEASUREMENTS FOR CONSTANT TRANSMITTED POWER

We first study the capacity dependence on distance for constant transmitted power.

A. Single Versus Hybrid Polarization Subsystems in the Hallway

We compare the single polarization 4×4 subsystems with the hybrid polarization 4×4 subsystem in the hallway environment. The results are shown in Fig. 5.

The first observation is that layouts I and II have very similar performances for both polarizations.

By comparison of the two plots, we can observe that the horizontally polarized subsystems achieve lower capacity than their vertically polarized counterparts, as one would expect because of the lower received signal power.

The HV subsystem outperforms the single-polarization subsystems in most locations, despite the fact that averaging the received power over both polarizations gives a value lower than the dominant (vertical) polarization alone. Coupling between polarizations is due to scattering from indoor clutter and oblique incidence on the walls. Therefore, it is a process independent of the same polarization coupling (which is due to regular incidence on the floor, the ceiling, and the walls) and achieves an added degree of freedom.

B. Single Versus Hybrid Polarization Systems

We repeat the above analysis for the labs. The added parameter is the antenna orientation.

Figs. 6 and 7 compare the single versus the hybrid polarization subsystems for the laboratory environment. As a reference the curves for the capacity of the hybrid polarization subsystem in the hallway have been added. The comparison with the hallway curves shows that the power loss incurred by going into the labs has a detrimental effect on the achievable capacity compared with that at similar distances in the hallway.

By comparison of the two sets of plots, we observe that the vertically and the horizontally polarized subsystems achieve similar capacities. Both polarizations have the same average received power, as the power analysis showed.

Any advantage in using combined polarization systems is due to multipath and in particular to the fact that the two polarizations get scattered locally in independent ways. The hybrid polarization subsystem performs only slightly better than the single polarization subsystems. This is consistent with rich scattering for same polarization coupling.

Similar results are observed for all antenna orientations. The advantage of using both polarizations is more pronounced for the 270° orientation of the antennas. In that case, the receivers are looking at the door and there is a significant path coming

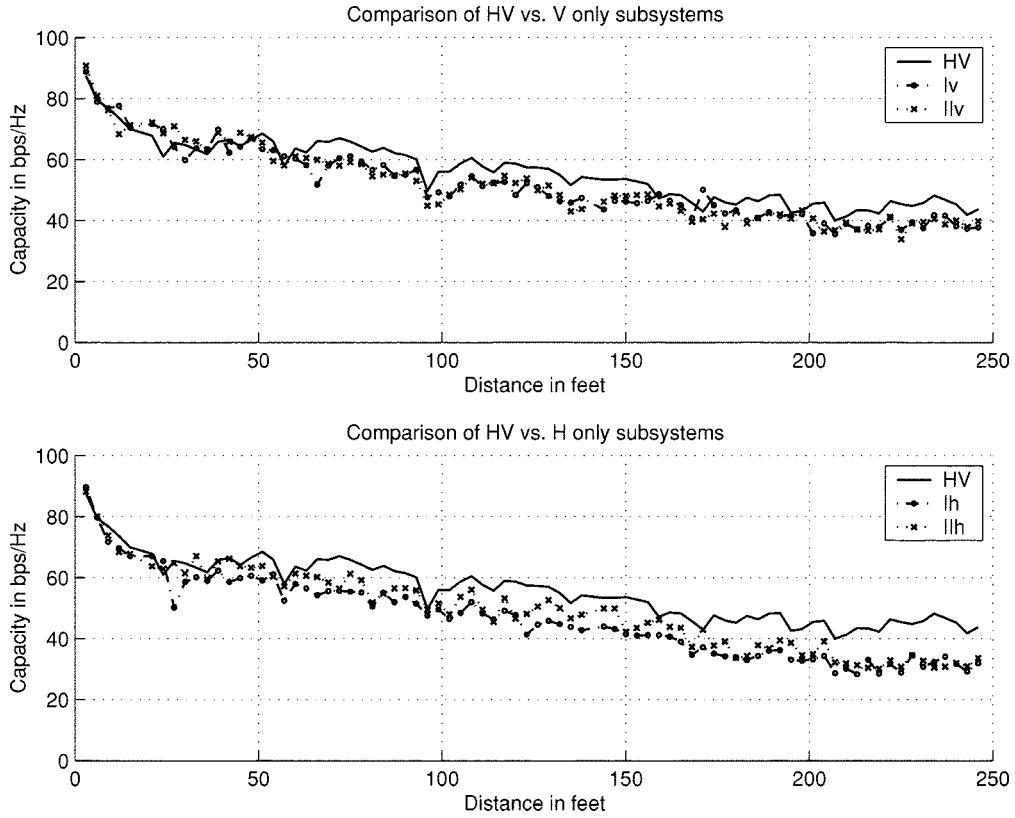

Fig. 5. Comparison of single versus hybrid polarization 4×4 subsystems for 0° oriented receivers in the hallway.

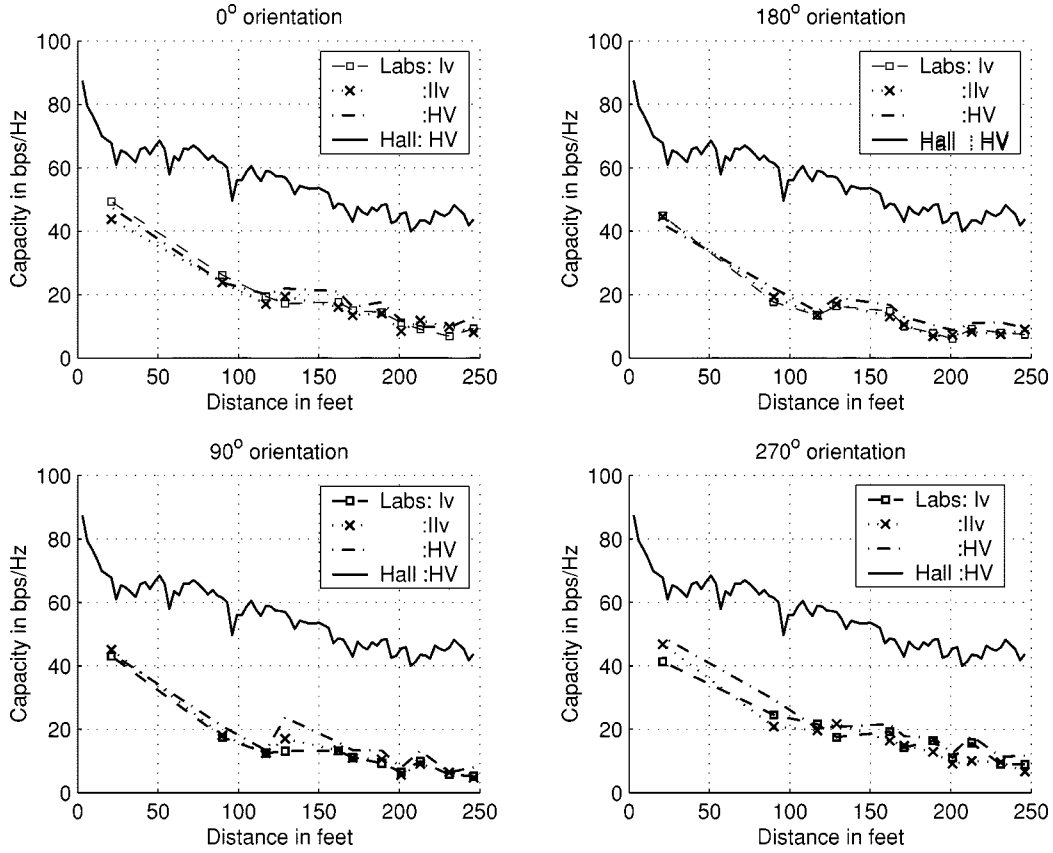

Fig. 6. Comparison of vertical versus hybrid polarization 4×4 subsystems in the labs.

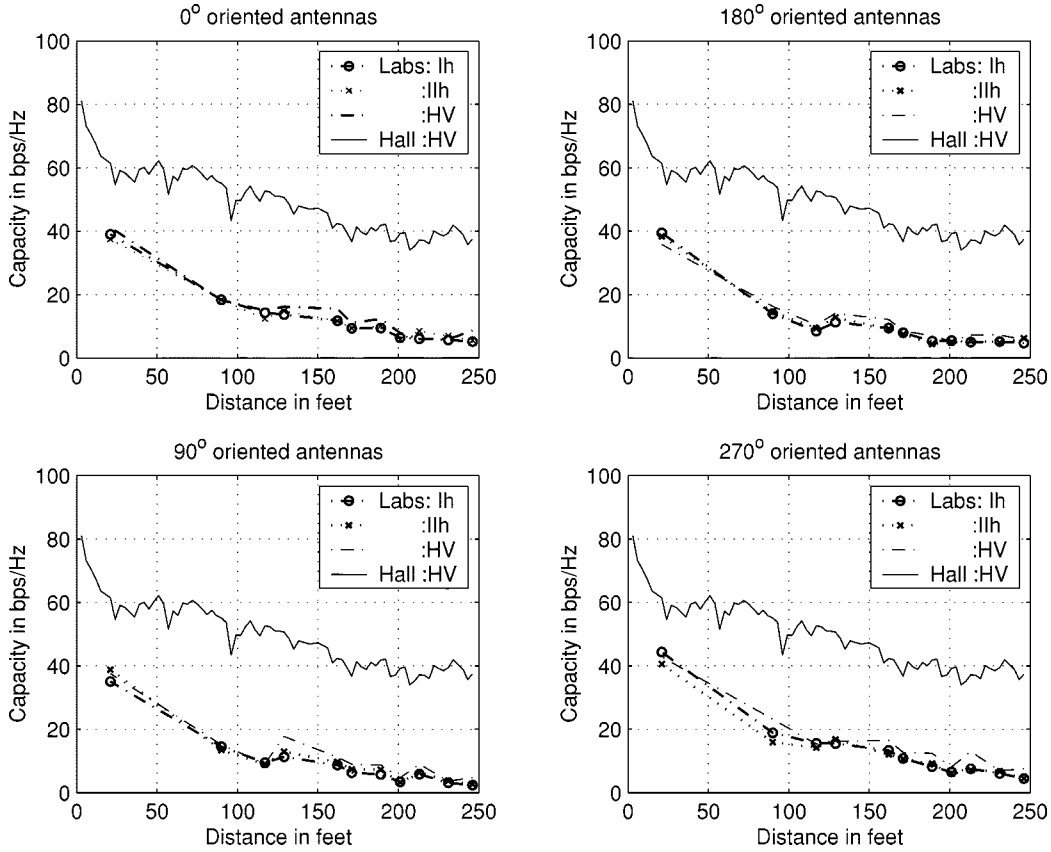

Fig. 7. Comparison of horizontal versus hybrid polarization 4×4 subsystems in the labs.

from that direction. This makes the channel gains for same-polarization coupling more correlated and limits the channel capacity.

All these effects are similar for both geometrical layouts.

VI. Capacity for Constant SNR

The above discussion incorporates the effect of both power rolloff and channel change with distance. To make the separation of the two effects obvious, we present the results for a constant SNR.

Following the analysis of Section II-D, we normalize the channel transfer matrix $\mathbf{T}$ by the average channel gain g. This defines the normalized channel transfer matrix $\mathbf{H}$ ($\mathbf{T} = g\mathbf{H}$). We then use (6) to calculate the channel capacity for a reference SNR ρ_{ref}. For our analysis the reference SNR is taken to be 20 dB ($\rho_{\mathrm{ref}} = 20$ dB), which is a reasonable value for a wireless system.

The maximum capacity that a 4×4 system at an average SNR of 20 dB ($= 100$) can achieve is

$$C_{\mathrm{MAX},4\times4} = 4\log_2(1+100) = 27 \text{ b/s/Hz}$$

under the normalization constraint that we have imposed $1/(NM)\sum_{i=1}^{N}\sum_{j=1}^{M}|H_{ij}|^2 = 1$.

This occurs when the normalized channel transfer matrix is unitary.

Another common point of reference is the capacity of a Gaussian channel, where the elements of the channel transfer matrix are complex independent Gaussian distributed random variables with variance one. In that case, the 50% and the 99% percentiles of the capacity distribution are

$$C_{50\%} = 22 \text{ b/s/Hz}$$
$$C_{99\%} = 25 \text{ b/s/Hz}.$$

A. Single Versus Hybrid Polarization Systems in the Hallway

We compare the single versus the hybrid polarization 4×4 subsystems in the hallway environment for a reference SNR of 20 dB. Fig. 8 shows the results of this comparison.

Both the hybrid and the single polarization subsystems (either layout) have a similar behavior with distance. At small distances, they display high capacity: the deterministic phases from each transmitter to each receiver antenna are very different due to the different path lengths. Although the amplitudes of the channel gains are similar, the phase differences are sufficient to provide rank of the channel transfer matrix greater than one. At large distances capacity is limited (about 50% of the maximum capacity). This indicates the limiting nature of the wireless channel in the hallway.

The hybrid polarization subsystem outperforms both the horizontally and the vertically polarized subsystems. None of the subsystems reaches the maximum capacity of 27 b/s/Hz. For some range of distances ($d < 90$ ft), the hybrid polarization subsystem outperforms the median capacity (22 b/s/Hz) of Gaussian channels. Any of the single polarization subsystems outperforms the median capacity (22 b/s/Hz) of Gaussian channels for some range of distances. The maximum distance for which this occurs varies between 10 ft and 50 ft depending on the choice of subsystem.

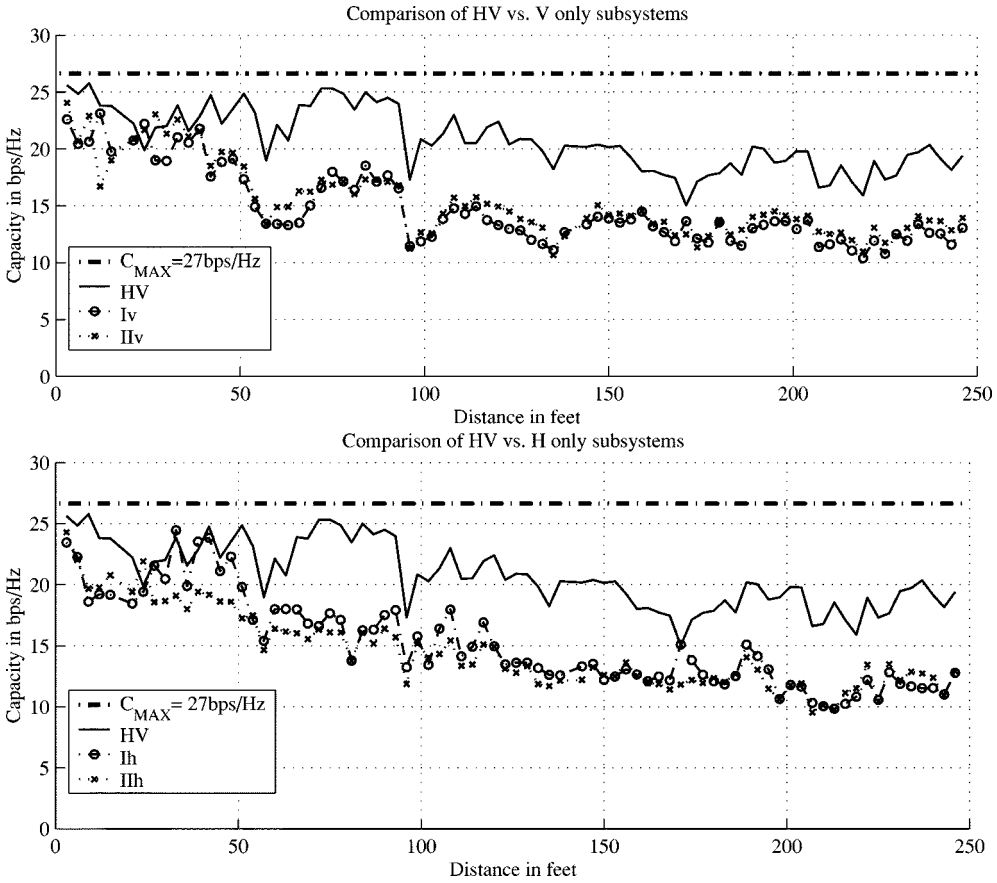

Fig. 8. Comparison of single versus hybrid polarization 4×4 subsystems for 0° oriented receivers in the hallway for the reference SNR $= 20$ dB.

B. Single Versus Hybrid Polarization Systems in the Labs

Figs. 9 and 10 show the corresponding results for the labs.

Layouts I and II behave in similar ways for both polarizations and for any antenna orientation.

The capacity in the labs for constant SNR is higher than the capacity at similar distances in the hallway, but similarly to the hallway results, the capacity for both the single and the hybrid polarization subsystems decays with distance. This can be explained as follows: at large distances the main propagation path is down the hallway and into the labs, where the signal gets scattered locally. However, the existence of a common propagation path results in high signal correlation and limits the channel capacity.

Also capacity decreases with distance more slowly for the hybrid polarization system. In particular for the 0° orientation, it stays approximately constant with distance.

None of the subsystems reaches the maximum capacity of 27 b/s/Hz (performance varies between 85% and 50% of the maximum depending on the location, the orientation, and the choice of subsystem), but again for some range of distances they outperform the median capacity of Gaussian channels.

VII. Conclusion

We have analyzed the behavior of a multiple element antenna system in an indoor environment based on the measurements taken in the Lucent Bells Labs building in Crawford Hill, NJ, with a system of 12 transmitters and 15 receivers. The parameters that we investigated were the distance between the transmitting and the receiving arrays, the polarization of the transmitting and receiving elements, and the propagation environment.

The analysis of the power rolloff versus distance clearly demonstrated the different power rolloff behavior in the hallway and in the labs and the different propagation characteristics of the horizontal versus the vertical electric field polarization. In the hallway, the power rolloff is better described by a distributed loss model ($e^{-\alpha d}$). There is little local scattering and the angular spread is limited (the LOS component is significant). Also the power of the horizontally polarized waves decays faster with distance than that of the vertically polarized fields and the cross-polarization coupling is about -15 dB. In the labs, the power rolloff behavior is described by a $d^{-\gamma}$ law and the angular spread is wider due to the rich local scattering. The two polarizations display similar rolloff behavior with distance and the cross-polarization coupling is about 0 dB. There is a loss of at least 15 dB in the labs relative to the hallway measurement at similar distances.

The analysis of the capacity behavior of the system with respect to polarization in the hallway showed that the capacity of horizontally polarized systems reflects the lower average received signal power. Hybrid polarization systems perform better than either single polarization system in terms of capacity due to the independence of the propagation paths for the two polarizations under either the constant transmitted power or the constant SNR assumption.

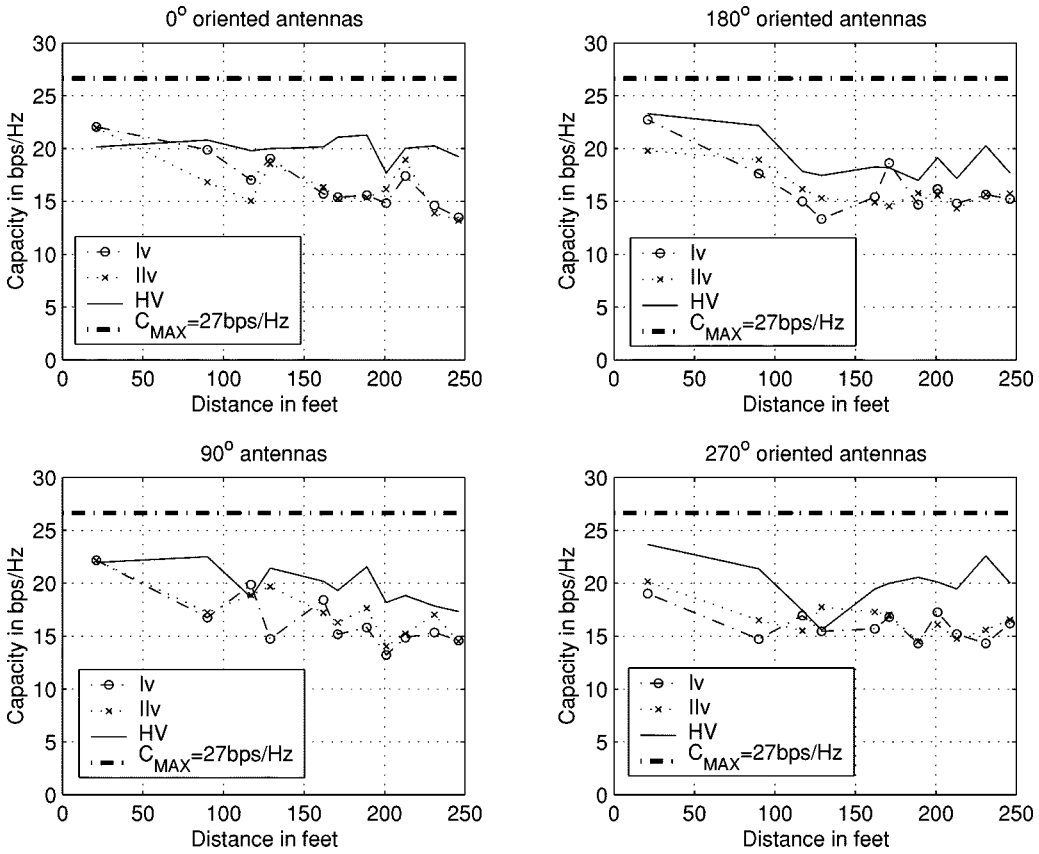

Fig. 9. Comparison of vertical versus hybrid polarization 4×4 subsystems in the labs for SNR $= 20$ dB.

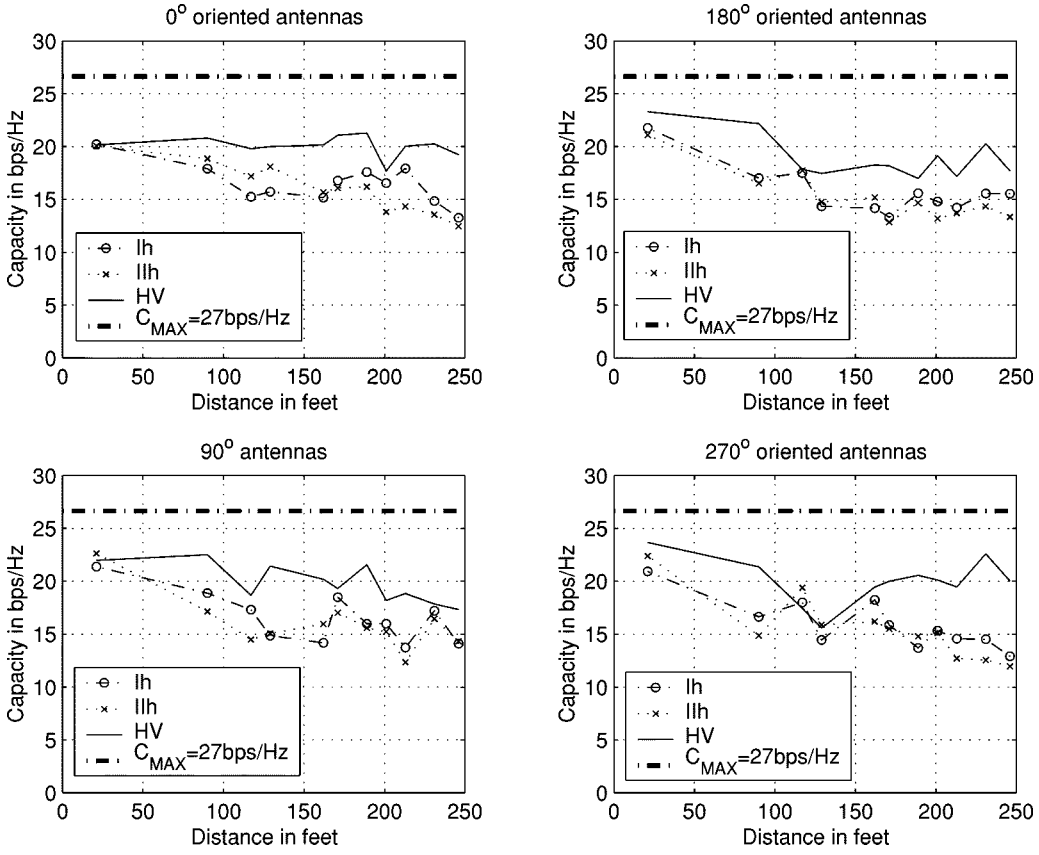

Fig. 10. Comparison of horizontal versus hybrid polarization 4×4 subsystems in the labs for SNR $= 20$ dB.

The analysis of the capacity behavior in the labs showed that the power loss is the most important effect that reduces the channel capacity. Under the assumption of constant SNR, the phenomenon that limits the channel capacity in the labs is the existence of a common propagation path (down the hallway and into the labs) that increases the signal correlation. These observations are independent of antenna orientation, which agrees with the rich local scattering assumption.

Finally, these results hold for all array layouts that we investigated, i.e., channel capacity is robust to small changes in the geometrical layout.

The conclusion that we draw is that there lies an advantage in using both electric field polarizations. However, there are environments, where the antenna placement and/or polarization is not the limiting factor in the capacity behavior of the system, but rather the channel itself is.

ACKNOWLEDGMENT

The set of measurements that has been presented was taken with the BLAST prototype built by G. Golden. The authors would like to thank M. Stoytchev for his invaluable help in taking the measurements. They specifically thank the Wireless Research Department for their patience and tolerance and the useful and stimulating discussions.

REFERENCES

[1] G. J. Foschini and M. J. Gans, "On limits of wireless communications in a fading environment when using multiple antennas," *Wireless Pers. Commun.*, vol. 6, pp. 311–335, Mar. 1998.

[2] P. W. Wolniansky, G. J. Foschini, G. D. Golden, and R. A. Valenzuela, "V-BLAST: An architecture for realizing very high data rates over the rich scattering wireless channel," in *Proc. ISSSE '98*, Sept. 1998, pp. 295–300.

[3] D. Chizhik, J. Ling, and R. A. Valenzuela, "The effect of electric field polarization on indoor propagation," in *Proc. Int. Conf. Universal Personal Communications '98 (ICUPC '98)*, 1998, pp. 459–462.

[4] P. Kyritsi, P. W. Wolniasnky, and R. A. Valenzuela, "Indoor BLAST measurements: Capacity of multi-element antenna systems," *Multi-Access, Mobility and Tele-Traffic for Wireless Communications*, pp. 60–49, Dec. 2000.

[5] D. M. J. Devarsivatham, "A comparison of time delay spread and signal level measurements within two dissimilar office buildings," *IEEE Trans. Antennas Propagat.*, vol. AP-35, pp. 319–324, Mar. 1987.

[6] T. L. Marzetta, "BLAST training: Estimating channel characteristics for high capacity space-time wireless," in *Proc. 37th Annu.l Allerton Conf. Communication, Control, Computing*, Monticello, IL, Sept. 22–24, 1999.

[7] P. Kyritsi, R. A. Valenzuela, and D. C. Cox, "Effect of channel estimation on the accuracy of capacity estimation," in *Proc. VTC 2001 Spring*, Rhodes, Greece, May 4–9, 2001.

[8] P. Kyritsi and D. C. Cox, "Propagation characteristics of horizontally and vertically polarized electric fields in an indoor environment," in *Proc. VTC 2001 Fall*, Atlantic City, NJ, 2001.

[9] D. P. McNamara, M. A. Beach, P. Karlsson, and P. N. Fletcher, "Initial characterization of multiple input- multiple output (MIMO) channels for space-time communication," in *Proc. VTC 2000 Fall*, Boston, MA.

[10] D. C. Cox, R. R. Murray, H. W. Arnold, A. W. Norris, and M. F. Wazowicz, "Cross-polarization coupling measured for 800 MHz radio transmission in and around houses and large buildings," *IEEE Trans. Antennas Propagat.*, vol. 34, pp. 83–88, Jan. 1986.

[11] H. W. Arnold, R. R. Murray, and D. C. Cox, "815 MHz radio attenuation measured within two commercial buildings," *IEEE Trans. Antennas Propagat.*, vol. 37, pp. 1335–1339, Jan. 1986.

[12] D. Gesbert, H. Bölcskei, D. Gore, and A. Paulraj, "MIMO wireless channels: Capacity & performance prediction," in *Proc. Globecom 2000*, vol. 2, Nov. 2000, pp. 1083–1088.

Persefoni Kyritsi (S'98) received the B.S. degree in electrical engineering from the National Technical University of Athens, Greece, in 1996, and the M.S. and Ph.D. degrees in electrical engineering from Stanford University, Stanford, CA, in 1998 and 2002, respectively.

She has worked in several aspects of wireless communications for Lucent Technologies Bell Labs, in wireline communications for Deutsche Telekom, Frankfurt, Germany, and in circuit design for Intel Corporation and the Nokia Research Center, Helsinki, Finland. She currently holds the position of Research Associate at the Center for PersonKommunikation in Aalborg University, Aalborg, Denmark. Her research interests include radio channel measurements, multiple antenna systems, radio propagation, and information theory for multiple-input/multiple-output systems.

Donald C. Cox (S'58–M'61–SM'72–F'79) received the B.S. and M.S. degrees in electrical engineering from the University of Nebraska, Lincoln, NE, in 1959 and 1960, respectively, and the Ph.D. degree in electrical engineering from Stanford University, Stanford, CA, in 1968.

From 1960 to 1963, he worked on microwave communications systems design at Wright-Patterson AFB, OH. From 1963 to 1968, he was at Stanford University working on tunnel diode amplifier design and research in microwave propagation in the troposphere. From 1968 to 1973, his research at Bell Laboratories, Holmdel, NJ, in radio propagation and on high-capacity radio systems provided important input to early cellular mobile radio system development and is continuing to contribute to the evolution of digital cellular radio, wireless personal communication systems, and cordless telephones. From 1973 to 1983, he was Supervisor of a group at Bell Laboratories, that did innovative propagation and system research for millimeter wave satellite communications. In 1978, he pioneered radio system and propagation research for low-power wireless personal communications systems. At Bell Laboratories, in 1983, he organized and became head of the Radio and Satellite Systems Research Department that became a Division in Bell Communications Research (Bellcore), with the breakup of the bell system on January 1, 1984. He was Division Manager of the Radio Research Division until it again became a department in 1991. He continued as Executive Director of the Radio Research Department where he championed, led, and contributed to research on all aspects of low-power wireless personal communications entitled Universal Digital Portable Communications (UDPC). He was instrumental in evolving the extensive research results into specifications that became the U.S. standard for the Wireless or Personal Access Communications System (WACS or PACS). In September 1983, he became a Professor of Electrical Engineering and Director of the Center for Telecommunications at Stanford University, where he continues to pursue research and teaching of wireless mobile and personal communications. He was appointed Harald Trap Friis Professor of Engineering, in 1994. He is author or coauthor of many papers and conference presentations, including many invited and several keynote addresses and books. He has been granted 15 patents.

Dr. Cox received an Honorary Doctor of Science from the University of Nebraska, in 1983. He was a Member of the Administrative Committee of the IEEE Antennas and Propagation Society (1986–1988) and an Associate Editor of the IEEE TRANSACTIONS ON ANTENNAS AND PROPAGATION (1983–1986). He is a member of the National Academy of engineering, a member of commissions B, C, and F of USNC/URSI, and was a member of the URSI Intercommission Group on Time Domain Waveform Measurements (1982–1984). He was awarded the IEEE 1983 Alexander Graham Bell Medal "For pioneering and leadership in personal portable communications" and was a corecipient of the 1983 International Marconi Prize in Electromagnetic Wave Propagation (Italy). He also received the IEEE 1985 Morris E. Leeds Award, the 1983 IEEE Vehicular Society Paper of the Year Award, the 1990 Communications Magazine Prize Paper Award, the Bellcore Fellow Award, in 1991, the IEEE Communications Society L.G. Abraham Prize Paper Award, in 1992, and the IEEE Third Millennium Medal, in 2000. He is a fellow of AAAS and the Radio Club of America. He is a member of Sigma Xi, Sigma Tau, Eta Kappa Nu, Phi Mu Epsilon, and is a Registered Professional Engineer in the states of Ohio and Nebraska.

Reinaldo A. Valenzuela (M'85–SM'89–F'99) received the B.S. degree from the University of Chile and the Ph.D. from the Imperial College of Science and Technology of the University of London, London, U.K.. His doctoral work introduced novel digital filters for transmultiplexers.

At Bell Laboratories, Holmdel, NJ, he studied indoor microwave propagation and modeling, packet reservation multiple access for wireless systems and optical WDM networks. He was manager, Voice Research Department at Motorola Codex, involved in the implementation of integrated voice and packet data systems. On returning to Bell Laboratories, he led a multidisciplinary team to create a software tool for Wireless System Engineering (WiSE), now in widespread use in Lucent Technologies. He is now head of the Wireless Communications Research Department, Lucent Technologies, Bell Labs Innovations, Holmdel, NJ. He is interested in microwave propagation measurements and models, third-generation wireless systems, and achieving high capacities employing transmit and receive antenna arrays. He has published over 60 papers and holds 10 patents.

Dr. Valenzuela received the Distinguished Member of Technical Staff Award from Lucent Technologies, Bell Labs Innovations.

Peter W. Wolniansky received the B.S.E.E. and M.S.E.E. degrees from Boston University, Boston, MA, in 1983 and 1986, respectively.

He performed system tests on the HAWK missile system for Raytheon Corporation, Bedford, MA, from 1983 to 1984 and studied optical data storage for Sony Corporation, Tokyo, Japan, from 1986 to 1987. Since 1988, he has worked for Lucent Technologies, Bell Labs Innovations, Holmdel, NJ as a Member of Technical Staff. His duties have included system engineering of modem networks, millimeter radio design, and propagation studies. His current activities include multichannel radio design and field studies using antenna arrays.